# Reverse time migration and Green's theorem: Part I- the evolution of concepts, and setting the stage for the new RTM method

**A. B. Weglein***, **R. H. Stolt**† **and J. D. Mayhan***

**M-OSRP, University of Houston,*

*617 Science & Research Bldg. 1, Houston, TX, 77004.*

†*ConocoPhillips,*

*600 North Dairy Ashford Road, Houston, TX 77079.*

(February 8, 2012)

**For Journal of Seismic Exploration**

Running head: **Wave-field representations using Green's theorem**

## ABSTRACT

In this paper, part I of a two paper set, we describe the evolution of Green's theorem based concepts and methods for downward continuation and migration. This forms the foundation and context for developing Greens theorem reverse time migration (RTM), in part II. We present the evolution of seismic exploration wave-field prediction models, as steps towards more completeness, consistency, realism and predictive effectiveness. Using simple and accessible analytic examples, we describe the difference between the need for subsurface information when the goal is a structure map, and contrast that with the case when the goal is both an accurate depth image and subsequent amplitude analysis at depth, that is, between migration and migration-inversion. The relationship between Green's theorem and the Lippmann Schwinger equation of scattering theory is used to help define the need behind the evolution of Green's theorem concepts and developments in seismic imaging, as well as providing a new insight for classic results like, *e.g.*, the Sommerfeld radiation condition. This paper provides a platform and detailed background for the second of this two paper set, where part II provides a new and consistent theory and method for RTM.

## INTRODUCTION

An important and central concept resides behind all current seismic processing methods that seek to extract useful subsurface information from recorded seismic data. That concept has two ingredients: (1) from the recorded surface seismic experiment and data, to predict what an experiment with a source and receiver at depth would record, and (2) exploiting the fact that a coincident source receiver experiment at depth, would, for small recording times, be an indicator of only local property changes at the coincident source-receiver position. These two ingredients, a wave-field prediction, and an imaging condition, reside behind all current leading edge seismic migration algorithms. The ultimate purpose of this two paper set is to advance our understanding, and provide concepts and new algorithms for the first of these two components: subsurface wave-field prediction from surface wave-field measurements. An accurate velocity model is required for this procedure to deliver an accurate structure map of boundaries in the subsurface where rapid changes in physical properties occur.

## OVERBURDEN INFORMATION FOR MIGRATION AND MIGRATION-INVERSION

In this paper, we show how to formulate and apply Green's theorem in an appropriate manner for one-way propagating waves. We begin with a simple discussion of back propagating waves and imaging to illustrate how the type of *a priori* information needed above a target reflector depends on our goal and level of information extraction, *e.g.*, about the location of and changes in physical properties across the target reflector. We show that only the velocity model above the reflector is needed to simply locate the reflector; whereas, all properties above the reflector are required if we want to determine both where any property has changed (structure imaging or migration) and what specific property has changed at the imaged reflector and by what amount (migration-inversion).

We begin by exemplifying how all traditional linear backpropagation methods for predicting waves at depth from surface reflection data need different types and degrees of *a priori* overburden subsurface information for different levels of ambition for subsurface target information extraction: migration *versus* migration-inversion. In traditional seismic processing, the spatial location of reflectors (migration) is determined by the velocity above the reflector while parameter estimation requires all properties above the depth image where changes in earth mechanical properties are to be determined. A very simple illustration of this idea can be obtained by using a 1D normal incident experiment using the model shown in Fig. 1, where $z_{ms}$ represents the depth of the source and receiver, and the depth of the first reflector is $z_1$, and the second reflector's depth is $z_2$, and $z_2$ is the location to be determined. The recorded data, $D(t)$, the wave-field at the coincident source and receiver position chosen as $z_{ms} = 0$, is given by

$$D(t, z_{ms} = 0) = R_1 \delta(t - 2t_1) + R'_2 \delta(t - 2t_2) \tag{1}$$

where $R_1 = R_{01}$ represents the reflection coefficient at the boundary between the first and second media, and $R'_2 = T_{01} R_{12} T_{10}$ represents the amplitude of the second event and is the composite transmission and reflection coefficient in the second medium. The two-way travel times for the first and second events are given by $2t_1$ and $2t_2$, respectively. Fourier transforming (1) gives

$$D(\omega, z_{ms} = 0) \quad = \quad R_1 e^{2i\omega t_1} + R_2' e^{2i\omega t_2} \tag{2}$$

where the first term on the right hand side is the primary from the first reflector (at $z = z_1$) and the second term is the primary from the second reflector (at $z = z_2$).

The next step is to locate the depth of the second reflector using the recorded data. To do so, we will call upon the simple solutions to the wave equation governing wave propagation in homogeneous media. In this example, that allows us to backpropagate separately the source and the receiver down reversing the actual propagation paths of the recorded upgoing waves. This step is known as downward continuation. Because, in traditional migration we assume that we know the velocity model above each reflector to be imaged, we will treat each primary separately, thus we write (2) as

$$D(\omega, z_{ms} = 0) = D_1(\omega, z_{ms} = 0) + D_2(\omega, z_{ms} = 0). \tag{3}$$

The source and receiver corresponding to the first primary,

$$D_1(\omega, z_{ms} = 0) = R_1 e^{2i\omega t_1} \tag{4}$$

are downward continued in the first medium (above the shallower reflector at $z_1$), giving

$$D_1(\omega, z) \quad = \quad R_1 e^{2i\omega t_1} e^{-2i \frac{\omega}{c_0} z}. \tag{5}$$

In the downward continuation for the first primary, we use the medium properties $(c_0, \rho_0)$ above that first reflector and the equation

$$\left( \frac{d^2}{dz^2} + \frac{\omega^2}{c_0^2} \right) D(\omega, z) = 0 \tag{6}$$

and, hence, the receiver and the source each contribute a factor of $e^{-i(\omega/c_0)z}$.

The solution in (5) simulates a coincident source and receiver reflection experiment at depth $z$. A non zero value of this coincident source and receiver experiment at depth at $t = 0^+$ indicates a reflector just below the coincident point in the medium. Hence, the next step in our example locates the reflectors by applying the imaging condition at $t = 0$ to the downward continued data. The latter is realized by integrating over all frequencies $\int d\omega \, D_1(\omega, z)$; in other words, we do an inverse Fourier transform evaluating the time in the exponential of the Fourier kernel with $t = 0$. Thus, we obtain

$$D_1(t = 0, z) = R_1 \delta(2t_1 - 2z/c_0), \tag{7}$$

corresponding to an image at $z = c_0 t_1$ at the depth of the first reflector. The second primary,

$$D_2(\omega, z_{ms} = 0) = R_2' e^{2i\omega t_2}, \tag{8}$$

is downward continued in the medium above the first reflector using the path of an upgoing wave satisfying the differential equation (6) and for the medium between the first and second reflector the equation used is

$$\left( \frac{d^2}{dz^2} + \frac{\omega^2}{c_1^2} \right) D(\omega, z) = 0, \tag{9}$$

which relates to the properties of the medium between $z_1$ and $z_2$. Therefore, taking the source and receiver to depth $z$ in the medium below the first reflector

$$
\begin{aligned}
D_2(\omega, z) &= D_2(\omega, z_{ms} = 0) e^{-i\frac{2\omega}{c_0}z_1} e^{-i\frac{2\omega}{c_1}(z-z_1)} \\
&= R_2' e^{2i\omega t_2} e^{-i\frac{2\omega}{c_0}z_1} e^{-i\frac{2\omega}{c_1}(z-z_1)},
\end{aligned}
\tag{10}
$$

and applying the imaging condition gives

$$
D_2(t=0, z) = R_2' \delta \left( 2t_2 - \frac{2z_1}{c_0} - \frac{2}{c_1}(z - z_1) \right). \tag{11}
$$

The second primary images at $z = z_1 + c_1(t_2 - t_1)$, the depth of the second reflector, $z_2$. Therefore the location depends only on the velocity above each reflector (and not on the density).

However, to determine changes in mechanical properties across each reflector requires the reflection coefficients $R_1$ and $R_{12}$ and the removal of $T_{01}T_{10}$ from $R_2'$ to determine $R_{12}$ where $R_2' = T_{01}R_{12}T_{10}$. To remove $T_{01}$ and $T_{10}$ we must know the changes in velocity and density at the first reflector. In other words, determining material property changes across each reflector requires the velocity and density (and absorption and all other property changes) above these two reflectors. The latter amplitude issue can be viewed as a consequence of the properties of the $R$'s and $T$'s which come from continuity conditions (note: the pressure and its normal derivative are not continuous when the density and velocity change across a boundary). If the latter continuity of pressure and its normal derivative were the case, then amplitude would only care about velocity changes, in this simple acoustic example. To determine the amplitude of a reflection coefficient at depth requires knowledge of all material properties above the reflector and not only velocity. That's worth keeping in mind for those pursuing/promoting 'true amplitude' migration, especially if non linear target identification is the ultimate goal. The general property of wave-field amplitude at depth from surface measurements follows from Green's theorem, where all medium properties are needed to provide the Green's functions in the medium, and necessary for determining the wave-field at depth.

## OVERVIEW ON THE EVOLUTION OF MIGRATION CONCEPTS AND GOALS: FROM NMO-STACK TO AVO AND MIGRATION TO MIGRATION-INVERSION, THE UNCOLLAPSED MIGRATION CONCEPT

As with all useful concepts, seismic migration has evolved and adapted to deal with ever more realistic and complex media and to allow higher and more ambitious goals for the imaged amplitudes. In seismic processing history the 'determine where anything changed' structure/migration people and their ideas/methods typically progressed totally independent from the 'what specifically changed' AVO people and their theories and methods. The AVO theorists and practitioners were never too concerned with locating the position in the earth of earth boundary changes, but rather focused on what specifically in detail was changing somewhere, and the migration people were not too interested in what was actually changing, after it was determined that something was changing at a point in the subsurface. Further, AVO people assumed a simple 1D earth and asked difficult, complex, detailed questions; while the structure seeking migration people assumed a complex multi-D earth and asked a less ambitious structure question 'where did anything change?' In the 1D world, NMO-stack evolved into AVO and multi-D migration evolved and was generalized into migration-inversion.

The two ingredients within wave equation migration are a backpropagation of waves and an imaging condition, where the latter imaging condition enables the backpropagated waves to be used to locate and delineate reflectors. The uncollapsed migration imaging principle introduced by Stolt, Clayton, and Weglein in the mid-1980's (Clayton and Stolt (1981), Stolt and Weglein (1985), and Weglein and Stolt (1999)) extended and generalized the earlier Claerbout coincident source and receiver at depth at time equals zero imaging condition. That earlier Claerbout principle imaging condition was aimed at producing a structure map. This paper advances the propagation component theory of the propagation-imaging principle duet and incorporates the Stolt-Clayton-Weglein uncollapsed migration imaging condition. That uncollapsed imaging condition remains the high water mark of imaging conditions today, allowing automatic amplitude analysis at depth with respect to the normal of the imaged reflector, or imaging and inverting a point diffractor. We will not progress the imaging condition in this two paper set. That uncollapsed migration time equals zero but non-coincident, (but proximal, by causality) source and receiver imaging condition has been reinvented (and sometimes relabeled), by among others Berkhout and Wapenaar (1988), de Bruin et al. (1990a), de Bruin et al. (1990b), Sava and Fomel (2006), and Sava and Vasconcelos (2009). Among recent contributions that have progressed seismic imaging conditions are: Vasconcelos et al. (2010), Sava and Vasconcelos (2010), and Douma et al. (2010).

We begin by discussing the history and evolution of models for the volume beneath the measurement surface within which we backpropagate surface reflection data.

## THE INFINITE HEMISPHERICAL MIGRATION MODEL

The earliest wave equation migration pioneers viewed the backpropagation region as an infinite hemispherical half space with known mechanical properties, whose upper plane surface corresponded to the measurement surface, as in, *e.g.*, Schneider (1978) and Stolt (1978). See Fig. 2.

There are several problems with the infinite hemispherical migration model. That model assumes: (1) that all subsurface properties beneath the measurement surface (MS) are known, and (2) that an anticausal Green's function (*e.g.*, Schneider (1978)), with a Dirichlet boundary condition on the measurement surface, would allow measurements (MS) of the wave-field, $P$, on the upper plane surface of the hemisphere to determine the value of $P$ within the hemispherical volume, $V$. The first assumption leads to the contradiction that we have not allowed for anything that is unknown to be determined in our model, since everything within the closed and infinite hemisphere is assumed to be known. Within the infinite hemispherical model there is nothing and/or nowhere below the measurement surface where an unknown scattering point or reflection surface can serve to produce reflection data whose generating reflectors are initially unknown and being sought by the migration process.

The second assumption, in early infinite hemispherical wave equation migration, assumes that Green's theorem with wave-field measurements on the upper plane surface and using an anticausal Green's function satisfying a Dirichlet boundary condition can determine the wave-field within $V$.

That conclusion assumes that the contribution from the lower hemispherical surface of $S$ vanishes as the radius of the hemisphere goes to infinity. That is not the case, as we explicitly demonstrate below. To examine the various large radius hemispherical surface contributions to Green's theorem wave prediction in a volume, it is instructive to review the relationship between Green's theorem and the Lippmann-Schwinger scattering equation.

## GREEN'S THEOREM REVIEW (THE LIPPMANN-SCHWINGER EQUATION AND GREEN'S THEOREM)

We begin with a space and time domain Green's theorem. Consider two wave-fields $P$ and $G_0$ that satisfy

$$(\nabla^2 - \frac{1}{c^2}\partial_t^2)P(\mathbf{r},t) = \rho(\mathbf{r},t) \tag{12}$$

$$\text{and } (\nabla^2 - \frac{1}{c^2}\partial_t^2)G_0(\mathbf{r},t,\mathbf{r}',t') = \delta(\mathbf{r}-\mathbf{r}')\delta(t-t'), \tag{13}$$

where we assume 3D wave propagation and the wavefield velocity $c$ is a constant. $\rho$ is a general source, *i.e.*, it represents both active sources (air guns, dynamite, vibrator trucks) and passive sources (heterogeneities in the earth). The causal solution to (12) can be written as

$$P(\mathbf{r},t) = \int_{-\infty}^{t^+} dt' \int_{\infty} d\mathbf{r}' \rho(\mathbf{r}',t') G_0^+(\mathbf{r},t,\mathbf{r}',t'), \tag{14}$$

where $G_0^+$ is the causal whole space solution to (13) and $t^+ = t + \epsilon$ where $\epsilon$ is a small positive quantity. The integral from $t^+$ to $\infty$ is zero due to the causality of $G_0^+$. Eq. (14) represents the linear superposition of causal solutions $G_0^+$ with weights $\rho(\mathbf{r}',t')$ summing to produce the physical causal wave-field solution to (12). Eq. (14) is called the scattering equation and represents an all space and all time causal solution for $P(\mathbf{r},t)$. It explicitly includes all sources and produces the field at all points of space and time. No additional boundary or initial conditions are required in (14).

Now consider the integral

$$\int_0^{t^+} dt' \int_V d\mathbf{r}' (P\nabla'^2 G_0 - G_0 \nabla'^2 P) = \int_0^{t^+} dt' \int_V d\mathbf{r}' \nabla' \cdot (P\nabla' G_0 - G_0 \nabla' P), \tag{15}$$

and we rewrite (15) using Green's theorem

$$\int_0^{t^+} dt' \int_V d\mathbf{r}' \nabla' \cdot (P\nabla' G_0 - G_0 \nabla' P) = \int_0^{t^+} dt' \int_S dS' \hat{n} \cdot (P\nabla' G_0 - G_0 \nabla' P). \tag{16}$$

This is essentially an identity, within the assumptions on functions and surfaces, needed to derive Green's theorem. Now choose $P = P(\mathbf{r}',t')$ and $G_0 = G_0(\mathbf{r},t,\mathbf{r}',t')$ from (12) and (13). Then replace $\nabla'^2 P$ and $\nabla'^2 G_0$ from the differential equations (12) and (13).

$$\nabla'^2 G_0 = \frac{1}{c^2}\partial_t'^2 G_0 + \delta(\mathbf{r}-\mathbf{r}')\delta(t-t') \tag{17}$$

$$\nabla'^2 P = \frac{1}{c^2}\partial_t'^2 P + \rho(\mathbf{r}',t'), \tag{18}$$

and assume that the out variables $(\mathbf{r},t)$ are in the intervals of integration: $\mathbf{r}$ in $V$, $t > 0$. The left hand side of (15) becomes:

$$\int_0^{t^+} dt' \int_V d\mathbf{r}' \frac{1}{c^2}(P\partial_{t'}^2 G_0 - G_0 \partial_{t'}^2 P) + P(\mathbf{r},t) - \int_0^{t^+} dt' \int_V d\mathbf{r}' \rho(\mathbf{r}',t') G_0(\mathbf{r},t,\mathbf{r}',t'). \tag{19}$$

The expression inside the first set of parentheses is a perfect derivative $\partial_{t'}(P\partial_{t'}G_0 - G_0\partial_{t'}P)$ integrated over $t'$. The result is (for $\mathbf{r}$ in $V$ and $t > 0$)

$$\begin{aligned} P(\mathbf{r},t) &= \int_V d\mathbf{r}' \int_0^{t^+} dt' \rho(\mathbf{r}',t') G_0(\mathbf{r},t,\mathbf{r}',t') - \frac{1}{c^2}\Big|_{t'=0}^{t^+} \int_V d\mathbf{r}' [P\partial_{t'}G_0 - G_0\partial_{t'}P] \\ &+ \int_0^{t^+} dt' \int_S dS' \hat{n} \cdot (P\nabla' G_0 - G_0 \nabla' P). \end{aligned} \tag{20}$$

We assumed differential equations (17) and (18) in deriving (20) and $G_0$ can be <u>any</u> solution of (17) in the space and time integrals in (15), causal, anticausal, or neither. Each term on the right hand side of (20) will differ with different choices of $G_0$, but the sum of the three terms will always be the same, $P(\mathbf{r},t)$.

If we now choose $G_0$ to be causal ($= G_0^+$) in (20), then in the second term on the right hand side the upper limit gives zero because $G_0^+$ and $\partial_{t'}G_0^+$ are zero at $t' = t^+$. The causality of $G_0^+$ and $\partial_{t'}G_0^+$ causes only the lower limit $t' = 0$ to contribute in

$$-\frac{1}{c^2}\Big|_{t'=0}^{t^+} \int_V d\mathbf{r}' [P\partial_{t'}G_0^+ - G_0^+\partial_{t'}P]. \tag{21}$$

If we let the space and time limits in (20) both become unbounded, *i.e.*, $V \to \infty$ and the $t'$ interval becomes $[-\infty, 0]$, and choose $G_0 = G_0^+$, the whole space causal Green's function, then by comparing (14) and (20) we see that for $\mathbf{r}$ in $V$ and $t > 0$ that

$$\int_{-\infty}^{t^+} dt' \int_S dS' \hat{n} \cdot (P\nabla' G_0^+ - G_0^+ \nabla' P) - \frac{1}{c^2}\Big|_{-\infty}^{t^+} \int_\infty d\mathbf{r}' [P\partial_{t'}G_0^+ - G_0^+\partial_{t'}P] = 0. \tag{22}$$

$V = \infty$ means a volume that spans all space, and $\infty - V$ means all points in $\infty$ that are outside the volume $V$. For $\mathbf{r}$ in $\infty$ and any time $t$ from (14) we get

$$\begin{aligned} P(\mathbf{r},t) &= \int_V d\mathbf{r}' \int_0^{t^+} dt' \rho(\mathbf{r}',t') G_0^+(\mathbf{r},t,\mathbf{r}',t') + \int_{\infty - V} d\mathbf{r}' \int_0^{t^+} dt' \rho(\mathbf{r}',t') G_0^+(\mathbf{r},t,\mathbf{r}',t') \\ &+ \int_V d\mathbf{r}' \int_{-\infty}^{0} dt' \rho(\mathbf{r}',t') G_0^+(\mathbf{r},t,\mathbf{r}',t') + \int_{\infty - V} d\mathbf{r}' \int_{-\infty}^{0} dt' \rho(\mathbf{r}',t') G_0^+(\mathbf{r},t,\mathbf{r}',t'). \end{aligned} \tag{23}$$

This equation holds for any $\mathbf{r}$ and any $t$.

For $\mathbf{r}$ in $V$ and $t > 0$ (23) and (20) must agree and

$$\begin{aligned} &- \frac{1}{c^2}\Big|_0^{t^+} \int_V d\mathbf{r}' [P\partial_{t'}G_0^+ - G_0^+\partial_{t'}P] \\ &= \int_V d\mathbf{r}' \int_{-\infty}^{0} dt' \rho(\mathbf{r}',t') G_0^+(\mathbf{r},t,\mathbf{r}',t') + \int_{\infty - V} d\mathbf{r}' \int_{-\infty}^{0} dt' \rho(\mathbf{r}',t') G_0^+(\mathbf{r},t,\mathbf{r}',t') \end{aligned} \tag{24}$$

and

$$\int_0^{t^+} dt' \int_S dS' \hat{n} \cdot [P\nabla' G_0 - G_0 \nabla' P] = \int_{\infty - V} d\mathbf{r}' \int_0^{t^+} dt' \rho(\mathbf{r}',t') G_0^+(\mathbf{r},t,\mathbf{r}',t'). \tag{25}$$

The solution for $P(\mathbf{r},t)$ in (14) expresses the fact that if all of the factors that both create the wave-field (active sources) and that subsequently influence the wave-field (passive sources, *e.g.*, heterogeneities in the medium) are explicitly included in the solution as in (20), then the causal solution is provided explicitly and linearly in terms of those sources, as a weighted sum of causal solutions, and no surface, boundary or initial conditions are necessary or required.

From (24) and (25) the role of boundary and initial conditions are clear. The contributions to the wave-field, $P$, at a point $\mathbf{r}$ in $V$ and at a time, $t$ in $[0, t^+]$ derives from three contributions: (1) a causal superposition over the sources within the volume $V$ during the interval of time, say $[0, t^+]$ and (2) initial conditions of $P$ and $P_t$ over the volume $V$, providing all contributions due to sources earlier than time $t' = 0$, both inside and outside $V$, to the solution in $V$ during $[0, t]$ and (3) a surface integral, enclosing $V$, integrated from $t' = 0$ to $t^+$ that gives the contribution from sources outside $V$ during the time $[0, t^+]$ to the field, $P$, in $V$ for times $[0, t^+]$. Succinctly stated, initial conditions provide contributions from sources at earlier times and surface/boundary conditions provide contributions from outside the spatial volume to the field in the volume during the $[0, t]$ time interval. If all sources for all space and all time are explicitly included as in (14), then there is no need for boundary or initial conditions to produce the physical/causal solution derived from a linear superposition of elementary causal solutions.

On the other hand, if we seek to find a physical causal solution for $P$ in terms of a linear superposition of anticausal solutions, as we can arrange by choosing $G_0 = G_0^-$ in (20), then the initial and surface integrals do <u>not</u> vanish when we let $V \to \infty$ and $[0, t] \to [-\infty, t]$. The vanishing of the surface integral contribution (as the radius of the surface $\to \infty$) to $P$ with the choice $G_0 = G_0^+$ is called the Sommerfeld radiation condition, and is readily understood by the comparison with (14).

In the $(\mathbf{r}, \omega)$ domain (12) and (13) become

$$(\nabla^2 + k^2)P(\mathbf{r}, \omega) = \rho(\mathbf{r}, \omega) \tag{26}$$

$$(\nabla^2 + k^2)G_0(\mathbf{r}, \mathbf{r}', \omega) = \delta(\mathbf{r} - \mathbf{r}'), \tag{27}$$

and the causal all space and time solution analogous to (14) is

$$P(\mathbf{r}, \omega) = \int_\infty d\mathbf{r}' \rho(\mathbf{r}', \omega) G_0^+(\mathbf{r}, \mathbf{r}', \omega), \tag{28}$$

and Green's second identity is

$$\int_V d\mathbf{r}' (P \nabla'^2 G_0 - G_0 \nabla'^2 P) = \oint_S dS' \, \hat{n} \cdot (P \nabla' G_0 - G_0 \nabla' P). \tag{29}$$

Substituting $\nabla^2 G_0 = -k^2 G_0 + \delta$ and $\nabla^2 P = -k^2 P + \rho$ in Green's theorem where $\int_{-\infty}^{\infty} P(\mathbf{r}, t) e^{i\omega t} dt = P(\mathbf{r}, \omega)$ we find

$$\int_V d\mathbf{r}' P(\mathbf{r}', \omega) \delta(\mathbf{r} - \mathbf{r}') = \int_V d\mathbf{r}' \rho(\mathbf{r}', \omega) G_0(\mathbf{r}, \mathbf{r}', \omega) + \oint_S dS' \hat{n} \cdot (P \nabla' G_0 - G_0 \nabla' P), \tag{30}$$

if $\mathbf{r}$ in $V$. There are no initial conditions, since in $\mathbf{r}, \omega$ we have already explicitly included <u>all</u> time in Fourier transforming from $t$ to $\omega$. All times of sources are included in the $(\mathbf{r}, \omega)$ domain. In $\mathbf{r}, \omega$ the issue is whether sources are inside or outside $V$. The Lippmann-Schwinger equation (28) provides the causal physical $P$ for all $\mathbf{r}$. Eq. (28) is the $\mathbf{r}, \omega$ version of (14) and must choose $G_0 = G_0^+$ (causal) to have $P$ as the physical solution built from superposition and linearity. In contrast, (30) (as in (20)) will produce the physical solution, $P$, with <u>any</u> solution for $G_0$ that satisfies (27).

Eq. (28) can be written as:

$$\int_V \rho G_0^+ + \int_{\infty - V} \rho G_0^+. \tag{31}$$

For $\mathbf{r}$ in $V$ the second term on the right hand side of (30) (with $G_0 = G_0^+$) equals the second term in (31), *i.e.*,

$$\int_{\infty - V} d\mathbf{r}' \rho G_0^+ = \oint_S dS' \hat{n} \cdot (P \nabla' G_0^+ - G_0^+ \nabla' P). \tag{32}$$

Thus, the first term in (31) gives contribution to $P$, for $\mathbf{r}$ in $V$ due to sources in $V$, and the second term in (31) gives contribution to $P$, for $\mathbf{r}$ in $V$ due to sources not in $V$. With $G_0 = G_0^+$

$$\oint_S dS' \hat{n} \cdot (P \nabla' G_0^+ - G_0^+ \nabla' P), \tag{33}$$

provides the contribution to the field, $P$, inside $V$ due to sources outside the volume $V$.

What about the large $|\mathbf{r}|$ contribution of the surface integral to the field inside the volume? We use Green's theorem to predict that the contribution to the physical/causal solution $P$ in $V$ from the surface integral in Green's theorem, in general, and also

$$\oint_S \{P \frac{\partial G_0^+}{\partial n} - G_0^+ \frac{\partial P}{\partial n}\} dS, \tag{34}$$

vanishes as $|\mathbf{r}| \to \infty$ and in contrast the contribution to $P$ in $V$ from

$$\oint_S \{P \frac{\partial G_0^-}{\partial n} - G_0^- \frac{\partial P}{\partial n}\} dS, \tag{35}$$

does not vanish as $|\mathbf{r}| \to \infty$.

We begin with (30)

$$P(\mathbf{r}, \omega) = \int_V d\mathbf{r}' \rho(\mathbf{r}', \omega) G_0^{\pm}(\mathbf{r}, \mathbf{r}', \omega) + \oint_S dS' \{P \frac{\partial G_0^{\pm}}{\partial n} - G_0^{\pm} \frac{\partial P}{\partial n}\} \qquad \mathbf{r} \text{ in V} \tag{36}$$

with $G_0$ either causal $G_0^+$ or anticausal $G_0^-$. When $|\mathbf{r}| \to \infty$, the contribution from the second term on the right hand side of (36) to $P$ in $V$ must go to 0 since

$$P(\mathbf{r}, \omega) = \int_\infty d\mathbf{r}' \rho(\mathbf{r}', \omega) G_0^+(\mathbf{r}, \mathbf{r}', \omega), \tag{37}$$

(the Lippmann-Schwinger equation). However, as $|\mathbf{r}| \to \infty$, with $G_0 = G_0^-$,

$$\oint_{S \to \infty} dS' \{P \frac{\partial G_0^-}{\partial n} - G_0^- \frac{\partial P}{\partial n}\} + \int_{V \to \infty} d\mathbf{r}' \rho(\mathbf{r}', \omega) G_0^-(\mathbf{r}, \mathbf{r}', \omega) = \int_{V \to \infty} d\mathbf{r}' \rho(\mathbf{r}', \omega) G_0^+(\mathbf{r}, \mathbf{r}', \omega) + 0, \tag{38}$$

so

$$\oint_{S \to \infty} \{P \frac{\partial G_0^-}{\partial n} - G_0^- \frac{\partial P}{\partial n}\} dS = \int_\infty [G_0^+(\mathbf{r}, \mathbf{r}', \omega) - G_0^-(\mathbf{r}, \mathbf{r}', \omega)] \rho(\mathbf{r}', \omega) d\mathbf{r}' \neq 0 \qquad \text{for all time.} \tag{39}$$

Hence, the large distance surface contribution to the physical field, $P$, within $V$ with the physical field $P$ and $P_n$ and an anticausal Green's function $G_0^-$ will not vanish as $|\mathbf{r}| \to \infty$. As we mentioned earlier, this is one of the two problems with the infinite hemisphere model of seismic migration.

Although

$$P(\mathbf{r}, \omega) = \int_\infty d\mathbf{r}' \rho(\mathbf{r}', \omega) G_0^-(\mathbf{r}, \mathbf{r}', \omega), \tag{40}$$

would be a solution to (12) and (26) for all $\mathbf{r}$, it would not be the causal/physical solution to (12) and (26). And hence, in summary the contribution to the causal/physical solution for $P(\mathbf{r}, \omega)$ for $\mathbf{r}$ in $V$ from

$$\int_S dS' \left( P \frac{dG_0^+}{dn} - G_0^+ \frac{dP}{dn} \right), \tag{41}$$

goes to zero as $|R| \to \infty$ where $P$ and $dP/dn$ corresponds to physical/causal boundary values of $P$ and $dP/dn$, respectively. Physical measurements of $P$ and $dP/dn$ on $S$ are always causal/physical values. The integral

$$\int_S dS' \left( P \frac{dG_0^-}{dn} - G_0^- \frac{dP}{dn} \right), \tag{42}$$

does not go to zero for anti-causal, $G_0^-$, and causal/physical $P$ and $dP/dn$. The latter fact bumps up against a key assumption in the infinite hemisphere models of migration. That combined with the fact the infinite hemisphere model assumes the entire subsurface, down to 'infinite' depth is known, suggests the need for a different model. That model is the finite volume model.

## FINITE VOLUME MODEL FOR MIGRATION

The finite model for migration assumes that we know or can adequately estimate earth medium properties (velocity) down to the reflector we seek to image. The finite volume model assumes that beneath the sought after reflector the medium properties are and remain unknown. The 'finite volume model' corresponds to the volume within which we assume the earth properties are known and within which we predict the wave-field from surface measurements. We have moved away from the two issues of the infinite hemisphere model, *i.e.*, (1) the assumption we know the subsurface to all depths and (2) that the surface integral with an anticausal Green's function has no contribution to the field being predicted in the earth.

The finite volume model takes away both assumptions. However, we are now dealing with a finite volume $V$, and with a surface $S$, consisting of upper surface $S_U$, lower surface $S_L$ and walls, $S_W$ (Fig. 3). We only have measurements on $S_U$. In the following sections on: (1) Green's theorem for one-way propagation; and (2) Green's theorem for two-way propagation we show how the choice of Green's function allows the finite volume migration model to be realized. The construction of the Green's function that allows for two-way propagation in $V$ is the new and significant contribution of this two paper set. It puts RTM on a firm wave theoretical Green's theorem basis, for the first time, with algorithmic consequence and consistent and realizable methods for RTM. The new Green's function is neither causal, anticausal, nor a combination of causal and/or anticausal, Green's functions. In the important paper by Amundsen (1994), a finite volume model for wave-field prediction is developed which requires knowing (*i.e.*, predicting through solving an integral equation) for the wave-field at the lower surface. In parts I and II we show that for one and two-way propagation, respectively, that with a proper and distinct choice of Green's function, in each case, that absolutely no wave-field measurement information on the lower surface is required or needs to be estimated/predicted. A major goal and contribution of this two paper set, is to show how to properly choose the Green's functions that allow for two-way propagation (for RTM application) without the need for measurements on the lower boundary of the closed surface in Green's theorem.

## FINITE VOLUME: ONE-WAY WAVE GREEN'S THEOREM DOWNWARD CONTINUATION

Consider a 1D up-going plane wave-field $P = Re^{-ikz}$ propagating upward through the 1D homogeneous volume without sources between $z = a$ and $z = b$ (Fig. 4). The wave $P$ inside $V$ can be predicted from

$$P(z,\omega) \ = \ \Big|_{z'=a}^{b} \{P(z',\omega)\ \frac{dG_0}{dz'}(z,z',\omega) - G_0(z,z',\omega)\frac{dP}{dz'}(z',\omega)\}, \tag{43}$$

with the Green's function, $G_0$, that satisfies

$$\left(\frac{d^2}{dz'^2} + k^2\right)\ G_0(z,z',\omega) \ = \ \delta(z - z'), \tag{44}$$

for $z$ and $z'$ in $V$. We can easily show that for an upgoing wave, $P = Re^{-ikz}$, that if one chooses $G_0 = G_0^+$ (causal, $e^{ik|z-z'|}/(2ik)$), the lower surface (i.e. $z' = b$) constructs $P$ in $V$ and the contribution from the upper surface vanishes. On the other hand, if we choose $G_0 = G_0^-$ (anticausal solution $e^{-ik|z-z'|}/(-2ik)$), then the upper surface $z = a$ constructs $P = Re^{-ikz}$ in $V$ and there is no contribution from the lower surface $z' = b$. This makes sense since information on the lower surface $z' = b$ will move with the upwave into the region between $a$ and $b$, with a forward propagating causal Green's function, $G_0^+$. At the upper surface $z' = a$, the anticausal $G_0^-$ will predict from an upgoing wave measured at $z' = a$, where the wave was previously and when it was moving up and deeper than $z' = a$.

Since in exploration seismology the reflection data is typically upgoing, once it is generated at the reflector, and we only have measurements at the upper surface $z' = a$, we choose an anticausal Green's function $G_0^-$ in one-way wave back propagation in the finite volume model. If in addition we want to rid ourselves of the need for $dP/dz'$ at $z' = a$ we can impose a Dirichlet boundary condition on $G_0^-$, to vanish at $z' = a$. The latter Green's function is labeled $G_0^{-D}$.

$$G_0^{-D} \ = \ -\frac{e^{-ik|z-z'|}}{2ik} - \left(-\frac{e^{-ik|z_I-z'|}}{2ik}\right) \tag{45}$$

where $z_I$ is the image of $z$ through $z' = a$. It is easy to see that $z_I = 2a - z$ and that

$$P(z) \ = \ -\frac{dG_0^{-D}}{dz'}(z,z',\omega)\Big|_{z'=a} P(a) \ = \ e^{-ik(z-a)}P(a), \tag{46}$$

in agreement with a simple Stolt FK phase shift for back propagating an up-field. Please note that $P(z,\omega) = -dG_0^{-D}/dz'(z,z',\omega)|_{z'=a}P(a,\omega)$ back propagates $P(z' = a,\omega)$, not $G_0^{-D}$. The latter thinking that $G_0^{-D}$ back propagates data is a fundamental mistake/flaw in many seismic back propagation migration and inversion theories.

The multidimensional 3D generalization for downward continuing both sources and receivers for an upgoing wave-field is as follows:

$$\begin{aligned} & \int \frac{dG_0^{-D}}{dz_s}(x'_s, y'_s, z'_s, x_s, y_s, z_s;\omega) \\ \times & \left[\int \frac{dG_0^{-D}}{dz_g}(x'_g, y'_g, z'_g, x_g, y_g, z_g;\omega) D(x'_g, y'_g, z'_g, x'_s, y'_s, z'_s;\omega) dx'_g dy'_g\right] dx'_s dy'_s \\ = & \ M(x_s, y_s, z_s, x_g, y_g, z_g;\omega) \\ = & \ M(x_m, y_m, z_m, x_h, y_h, z_h;\omega), \end{aligned} \tag{47}$$

where $x_g + x_s = x_m$, $y_g + y_s = y_m$, $z_g + z_s = z_m$, $x_g - x_s = x_h$, $y_g - y_s = y_h$, and $z_g - z_s = z_h$. The uncollapsed migration is $M(x_m, y_m, z_m, x_h, y_h, z_h = 0; t = 0)$ and is ready for subsequent AVO analysis in a multi-D subsurface (see *e.g.* Clayton and Stolt (1981), Stolt and Weglein (1985), Weglein and Stolt (1999)).

In part II of this paper we examine Green's theorem for two-way RTM in a 1D and multi-D earth.

## COMMENTS/SUMMARY

In this paper, we have provided an overview of the evolution of migration models for one-way wave propagation, viewed as a progression of wave-field prediction from the perspective of Green's theorem concepts and methods. This provides a platform, background and context for wave-field prediction for RTM, the subject of part II of this two paper set.


## ACKNOWLEDGEMENTS

We thank the M-OSRP sponsors, NSF-CMG award DMS-0327778 and DOE Basic Sciences award DE-FG02-05ER15697 for supporting this research. R. H. Stolt thanks ConocoPhillips for permission to publish. We thank Lasse Amundsen of Statoil and Adriana Ramírez and Einar Otnes of WesternGeco for useful discussions and suggestions regarding RTM. We thank Xu Li, Shih-Ying Hsu, Zhiqiang Wang and Paolo Terenghi of M-OSRP for useful comments and assistance in typing the manuscript.

## REFERENCES


Amundsen, L., 1994, The propagator matrix related to the Kirchhoff-Helmholtz integral in inverse wavefield extrapolation: Geophysics, **59**, 1902–1910.

Berkhout, A. J., and C. P. A. Wapenaar, 1988, Delft philosophy on inversion of elastic data, *in* 58th Annual International Meeting, SEG, Expanded Abstracts: Soc. Expl. Geophys., **7**, 831–833.

Clayton, R. W., and R. H. Stolt, 1981, A Born-WKBJ inversion method for acoustic reflection data: Geophysics, **46**, 1559–1567.

de Bruin, C. G. M., C. P. A. Wapenaar, and A. J. Berkhout, 1990a, Angle-dependent reflectivity by means of prestack migration: Geophysics, **55**, 1223–1234.

———, 1990b, Imaging for angle-dependent reflectivity in the presence of dip, *in* 60th Annual International Meeting, SEG, Expanded Abstracts: Soc. Expl. Geophys., **9**, 1503–1506.

Douma, H., D. Yingst, I. Vasconcelos, and J. Tromp, 2010, On the connection between artifact filtering in reverse-time migration and adjoint tomography: Geophysics, **75**, S219–S223.

Sava, P., and S. Fomel, 2006, Time-shift imaging condition in seismic migration: Geophysics, **71**, S209–S217.

Sava, P., and I. Vasconcelos, 2009, Efficient computation of extended images by wavefield-based migration, *in* 79th Annual International Meeting, SEG, Expanded Abstracts: Soc. Expl. Geophys., **28**, 2824–2828.

———, 2010, Extended imaging conditions for wave-equation migration: Geophysical Prospecting. (in press).

Schneider, W. A., 1978, Integral formulation for migration in two and three dimensions: Geophysics, **43**, 49–76.

Stolt, R. H., 1978, Migration by Fourier transform: Geophysics, **43**, 23–48.

Stolt, R. H., and A. B. Weglein, 1985, Migration and inversion of seismic data: Geophysics, **50**, 2458–2472.

Vasconcelos, I., P. Sava, and H. Douma, 2010, Nonlinear extended images via image-domain interferometry: Geophysics, **75**, SA105–SA115.

Weglein, A. B., and R. H. Stolt, 1999, Migration-inversion revisited (1999): The Leading Edge, **18**, 950–952, 975.

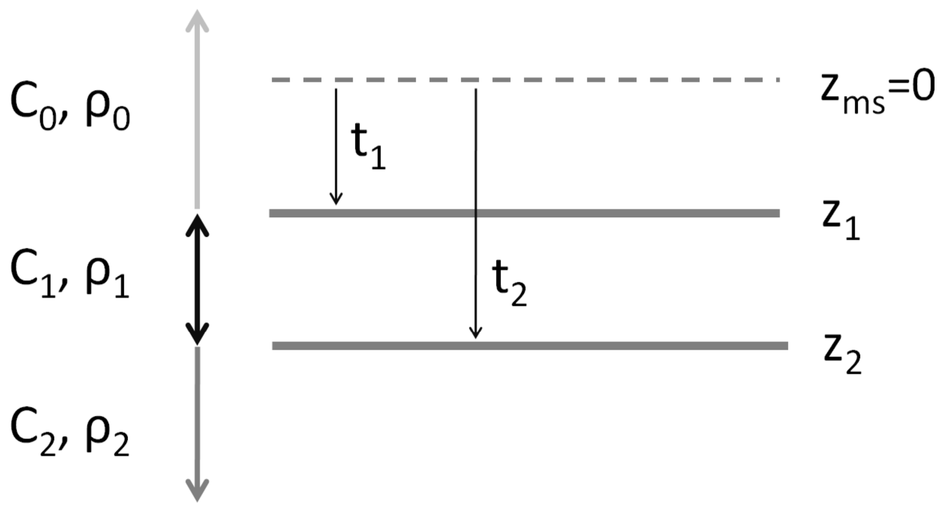


**Figure 1:** *Zero-offset model. The velocity is denoted by c, and the density by ρ.*

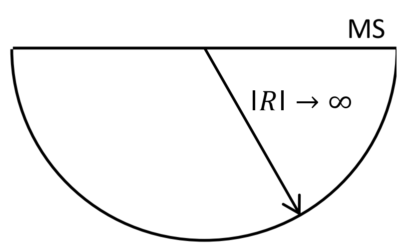


**Figure 2:** *The infinite hemispherical migration model. The measurement surface is denoted by MS.*

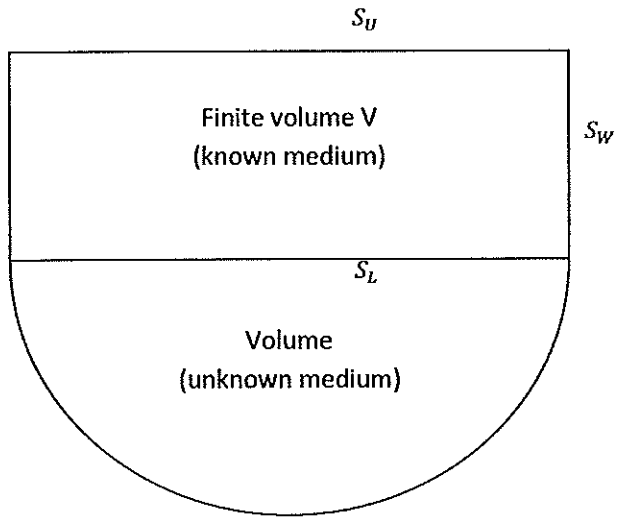


**Figure 3:** *A finite volume model*

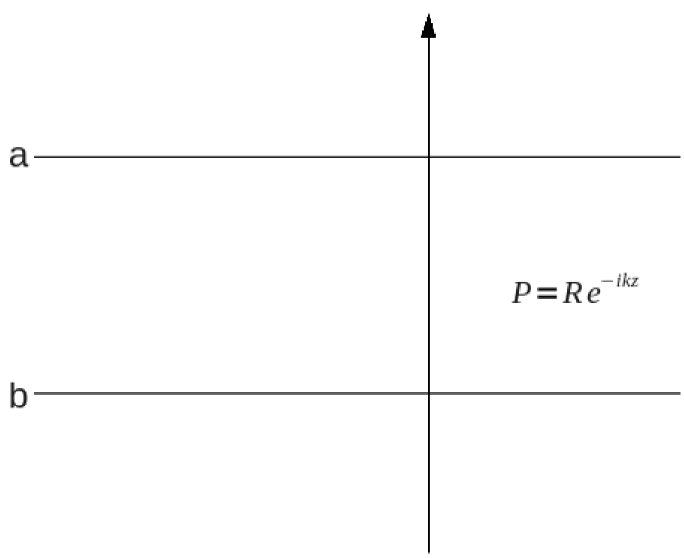


**Figure 4:** *1D up-going plane wave-field*